Atmósfera (1998) 11, pp. 173-197

Barotropic eulerian residual circulation in the Gulf of California due to the M_2 tide and wind stress

M. L. ARGOTE, M. F. LAVIN and A. AMADOR

CICESE, Departamento de Oceanografía Física, Apdo. Postal 2732, Ensenada, Baja California, México

(Manuscript received March 10, 1997; accepted in final form Feb. 2, 1998)

RESUMEN

Se emplea un modelo numérico de diferencias finitas, no-lineal e integrado verticalmente, para analizar dos mecanismos de forzamiento de la circulación barotrópica del Golfo de California: la rectificación topográfica de la corriente de marea (M_2) y el esfuerzo del viento. Los términos no-lineales de las ecuaciones de momento producen una distribución desorganizada de fuertes corrientes residuales inducidas por la marea ($u_e > 5$ cm s^{-1}) en los canales del archipiélago central y en el Golfo Norte una circulación anticiclónica a lo largo de las isobatas con velocidades de $u_e < 2.5$ cm s^{-1} en el borde de la Cuenca Delfín. Estos resultados numéricos concuerdan con resultados analíticos, los cuales indican que los términos advectivos de las ecuaciones de momento son responsables del flujo medio inducido por la marea y además que el efecto combinado del término de Coriolis (regulado por fricción en el fondo) y condiciones de continuidad producen flujo a lo largo de las isobatas.

El término de fricción únicamente juega un papel importante en la generación de corrientes residuales inducidas por la marea en la zona somera del delta del Río Colorado. El efecto del esfuerzo del viento fue simulado incluyendo en el modelo un esfuerzo superficial constante ($\tau = 0.016$ Pa): del NO para las condiciones de invierno y del SE para las de verano. La circulación inducida por el viento fue obtenida promediando sobre un ciclo de marea y restando las residuales inducidas por la marea. Las dos direcciones de viento producen distribuciones espaciales de corrientes casi idénticas, pero con direcciones opuestas.

Los principales rasgos de la circulación, inducidos por viento del NO son: (a) En el Golfo Norte, giros anticiclónicos con corrientes intensas (de hasta ~10 cm s^{-1}) a lo largo de las isobatas sobre los bordes de cuencas de Delfín y Wagner y a lo largo de la costa este, frente a las bahías de Adair y San Jorge. Se aprecia un flujo a lo largo de la costa de la península, desde la desembocadura Río Colorado hasta Bahía San Luis Gonzaga. (b) En el Golfo Sur se aprecia un flujo intenso (~10 cm s^{-1} a 15 cm s^{-1}) hacia el SE, restringido a la plataforma continental a lo largo de la costa continental; un flujo de retorno no tan claramente definido y menos intenso (5 cm s^{-1}), desde Santa Rosalía hasta Isla San Lorenzo producen una circulación anticiclónica al sur de las islas. Algunos rasgos de la circulación inducida por el viento concuerdan cualitativamente con observaciones de correntímetros, pero el modelo subestima la rapidez de las corrientes, lo cual puede ser atribuido a la baroclinicidad, la cual no se incluye en la simulación numérica.

ABSTRACT

A vertically integrated, non-linear numerical model in finite differences is used to analyze two forcing mechanisms of the mean barotropic circulation in the Gulf of California: topographic rectification due to tidal currents (M_2) and wind stress. Under tidal forcing the nonlinearities of the momentum equations induce unorganized strong tidal induced residual currents ($u_e > 5$ cm s^{-1}) in the channels between the islands, and along-isobath anticyclonic circulation in the Northern Gulf, with speeds $u_e < 2.5$ cm s^{-1} over the edge of Delfín Basin. These numerical results are in agreement with analytical results, which indicate that the tidal-induced currents are mostly due to the advective terms, and that continuity and the Coriolis term (but regulated by bottom friction) are responsible for the along-isobath flow.

The quadratic bottom friction plays a role in generating mean currents only in the very shallow area off the Colorado River Delta. The effect of wind stress was modeled by imposing upon the running M_2 model a constant surface stress (τ = 0.016 Pa), from the NW for winter conditions and from the SE for summer conditions. The wind-induced circulation was obtained by averaging over a tidal cycle and then subtracting the tidal residuals. The two wind directions produce almost identical circulation patterns, but with opposite directions.

For the NW wind stress, the main features of the predicted circulation are: (a) In the Northern Gulf an anticyclonic circulation pattern, with the strongest currents (up to $\sim$ 10 cm s^{-1}) following the bathymetry of the rim of Delfín Basin, Wagner Basin and the mainland coast off Bahía Adair and Bahía San Jorge. There is also a southward flow along the peninsula coast, from the Colorado River to Bahía San Luis Gonzaga. (b) In the Southern Gulf, there is a strong flow ($\sim$ 10 to 15 cm s^{-1}) to the SE over the continental shelf along the mainland coast. A somewhat less well-defined return flow ($\sim$ 5 cm s^{-1}) from Santa Rosalía to Isla San Lorenzo complete an anticyclonic circulation in the area immediately to the SE of the islands. Some of the predicted features of the wind-driven flow in the Northern Gulf of California are in qualitative agreement with current meter observations, but the model underestimates them which may be attributable to baroclinity, not included in the model.

1. Introduction

The Gulf of California (GC), located on the Northwestern Pacific coast of Mexico (Fig. 1), consists of a sequence of basins with depths increasing from ~200 m in its closed NW end, to ~3,500 m in the SE, where the gulf is in open communication with the Pacific Ocean. The GC is about 100 to 150 km wide, and is constrained by the Mexican mainland and by the peninsula of Baja California, which has a length of about 1200 km. At approximately two thirds of the open end, its cross-sectional area is drastically reduced by the presence of an archipelago, which is a transition zone between the shallow northern region and the deeper southern part of the gulf. In this paper we will refer to the area located to the NW of the archipelago as the Northern Gulf, and the area to the SE of the archipelago will be referred to as the Southern Gulf. The term Upper Gulf is used for the triangular area with vertices at the Colorado River, at San Felipe and at Puerto Peñasco (Fig. 1). The Northern Gulf presents a wide continental shelf. In contrast in the Southern Gulf the continental shelf is almost non-existent along the peninsula of Baja California, and it is ~30 km wide along the Mexican mainland.

The pattern of mean circulation, of the GC is still not well known. Although several features of the circulation of the gulf have been described from indirect evidence like; hydrographic data (Roden, 1964; Rosas-Cota, 1976; Bray, 1988 a, b; Fernández-Barajas *et al.*, 1994), satellite images (Lepley *et al.*, 1975; Badan-Dangon *et al.*, 1985; Paden *et al.*, 1991), sea surface tilt (Roden, 1964; Ripa, 1990) and from numerical modeling (Dressler, 1981; Quirós *et al.*, 1992; Carbajal, 1993; Beier, 1997), direct current observations have so far not been available to support any of the descriptions or models. Recent reviews of this subject are those of Badan-Dangon *et al.* (1991a) and Bray and Robles (1991).

In the Northern Gulf, the dominant water motions are tidal currents (Argote *et al.*, 1995). In this region surface current amplitudes up to 1.3 m s^{-1} have been measured over the shallow coastal band adjacent to the Colorado River Delta (Thomson *et al.*, 1969). In the channels of the archipelago, direct measurements by ship drift and radio buoys have also indicated the presence of energetic currents (1 to 3 m s^{-1}; Roden, 1964; Alvarez-Sánchez *et al.*, 1984). In Ballenas Channel, the currents are dominated by along-channel tidal oscillations with superimposed small-scale eddies (Alvarez-Sánchez *et al.*, 1984). Previous numerical models (Quirós *et al.*, 1992; Carbajal, 1993; Marinone, 1997) suggest that flow induced by the interaction of the tidal currents with the bathymetry occurs mainly on the archipelago, and in the Northern Gulf.

In the Southern Gulf, the mean surface current is apparently in phase with the wind direction (which is highly polarized along the gulf), with an inward flow in spring and summer and an

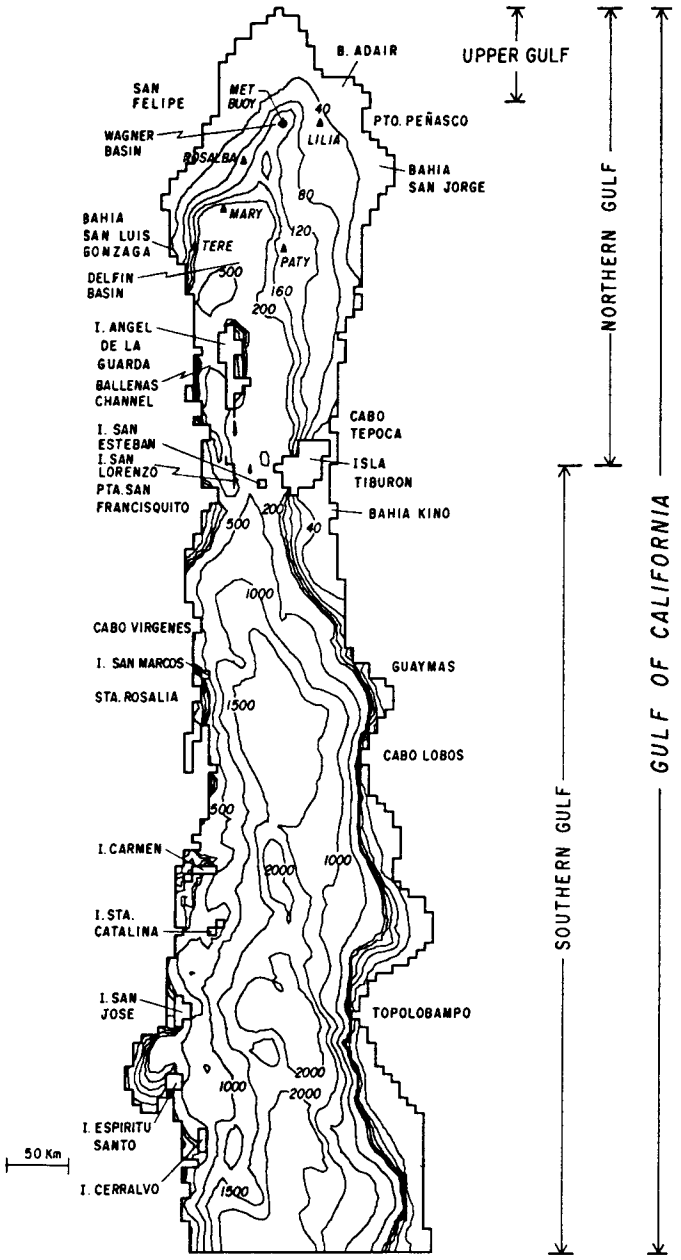

Fig. 1. The Gulf of California: model grid, digitized bathymetry, and nomenclature used. The triangles show the sites where current meter data were collected (Table 1).

outward flow in autumn and winter (Rosas Cota, 1976; Bray, 1988a, Ripa, 1990, 1997). The circulation in the Southern Gulf seems to be mostly geostrophic, with basin-wide gyres over the main basins (Emilsson and Alatorre, 1979; Fernández-Barajas *et al.*, 1994). The surface velocity is weaker in the Southern Gulf than in the Northern Gulf, with maximum velocities of about 15 cm s^{-1} (Roden, 1964; Rosas Cota, 1976).

The general features of the circulation in the gulf are likely to correspond to those observed in other continental shelves or semi enclosed basins, where mean or residual movements arise from

horizontal density gradients, externally imposed sea surface slopes, and from wind and tidal forcing. The relative importance of the possible driving mechanisms may change with location and with the seasons.

This paper assesses the role of tidal and winds forcing on the mean barotropic circulation of the Gulf of California. A vertically integrated non-linear hydrodynamical numerical model is used, and the results of the simulations for the Northern Gulf are supported by direct observations with several simultaneous short-term current meter arrays, and with Lagrangian drifters.

2. The model

The non-linear numerical model used here was developed by Hunter (1980), and its application to the M_2 tide in the Gulf of California (using a 6.6 km × 6.6 km grid, Fig. 1) has been described in some detail by Argote *et al.* (1995). The numerical model solves the depth-averaged shallow water equations of motion and the equation of continuity:

$$\frac{\partial \mathbf{u}}{\partial t} = -\mathbf{u}.\nabla\mathbf{u} - g\nabla\eta - f(\mathbf{k}\times\mathbf{u}) + \frac{\tau_w - \tau_b}{\rho_w(h+\eta)} + K_h(\nabla_h^2\mathbf{u}) \tag{1}$$

$$\frac{\partial \eta}{\partial t} + \nabla.[\mathbf{u}(h+\eta)] = 0 \tag{2}$$

where $\mathbf{u}$ is the vertically averaged horizontal velocity with components u and v in a Cartesian system with coordinates x and y.

$$\mathbf{u} \equiv \frac{1}{h+\eta}\int_{-h}^{\eta} \mathbf{u}_h(z)dz, \tag{3}$$

here z is positive upward from the free surface, and $\mathbf{u}_h(z)$ is the local horizontal component of the velocity at height z.

The relationships used for the wind stress (τ_w) and bottom stresses (τ_b) are:

$$\tau_w = \rho_a C_{10} \mid \mathbf{w}_{10} \mid \mathbf{w}_{10} \qquad \text{and} \qquad \tau_b = \rho_w C_d \mid \mathbf{u} \mid \mathbf{u}, \tag{4}$$

where $\mathbf{w}_{10}$ is the wind velocity at a high of 10 m. The definitions of the symbols and the numerical value of the coefficients used are given in: List of symbols

In general the model solves the vertically integrated equations using a staggered grid. The surface elevations and the two velocity components are computed at three different points. The finite difference scheme is an explicit leapfrog type. Along land boundaries the velocity normal to the coast is zero. On the open boundaries the tidal elevation and phase must be specified.

The model ran under the following assumptions: the Coriolis parameter f was held constant (7.7×10^{-5} s^{-1}), and the diffusion term was set at 10^2 m^2 s^{-1}. Given the grid size, a time step of $\nabla t = 12.42$ s was chosen to satisfy the Courant-Friedrich-Lewy stability requirement. The bottom drag coefficient ($C_d = 3.7\ 10^{-3}$) was chosen by running the model with different values until it produced the best agreement to the M_2 elevation amplitude in sampled stations in the Northern Gulf reported by (Gutiérrez and Morales, 1986).

3. Tidal-induced residual circulation

In this case the wind stress term (τ_w) of equation (1) was not included. The M_2 tide of the Gulf of California was modeled as a co-oscillating tide of a barotropic water body generated by the incoming tidal wave of the Pacific Ocean. At the open sea boundary the M_2 tidal elevations was prescribed according to observed amplitudes and phases

$$\eta = A\cos(\sigma t - \phi)$$

were A is amplitude, σ is angular frequency of the M_2 tide and ϕ is phase. The harmonic constants were obtained from Gutiérrez and Morales (1986).

In order to compare the tidal-induced residual flow generated by the model with direct measurements obtained by current meter, the Eulerian residual flow was obtained. Once the tidal solution of the model had converged (23 tidal cycles) and the residual flow pattern had achieved steady state. The Eulerian residual current was estimated by averaging the horizontal flow $\mathbf{u}$ over a complete time period T, following the definitions of Tee (1976) and Pingree and Maddock (1977).

$$\mathbf{u}_e = \frac{1}{T}\int_o^T \mathbf{u}dt \tag{5}$$

The dominance of the advective terms of the momentum equations in the generation of residual flow is made evident by contrasting the $\mathbf{u}_e$ distribution obtained from the linearized version of the model (Fig. 2a) against that with the fully non-linear model (Fig. 2b). Only in the Upper Gulf and in Adair Bay are there residual flows that may be associated to the bottom friction term and to the shape of the coast (Fig. 2a).

The strongest flow ($\mathbf{u}_e > 5$ cm s^{-1}) predicted by the full model is in the channels of the archipelago (Fig. 2b). Slower flow ($\mathbf{u}_e < 2.5$ cm s^{-1}) is predicted in the Northern Gulf, and it is almost negligible ($\mathbf{u}_e < 0.5$ cm s^{-1}) in the Southern Gulf.

North of the archipelago the flow is anticyclonic and along the isobaths, with stronger velocities in areas of pronounced depth gradients (along the rim of Delfín Basin, where $\mathbf{u}_e$ reaches a maximum of ~2.5 cm s^{-1}). The exception to the along-isobath flow occurs in the Upper Gulf, where a weak (0.5 cm s$^{-1} \leq \mathbf{u}_e \leq 1$ cm s^{-1}) southward flow occurs along the central axis of the Gulf. This southward flow appears to be associated to the convergence of two mesoscale eddies (~30 km diameter), rotating in opposite sense in the Upper Gulf. Clockwise eddies of similar diameter are also predicted in Adair Bay and near Puertecitos.

In the archipelago, the steep bottom slope and the complex geometry of the coastline, appear to be responsible for the generation of the strongest currents. Although the flow seems disorganized, a blow-up of the area (Fig. 2c) shows mesoscale eddies in the vicinity of coastal headlands, like the northern end of Angel de la Guarda Island, NW of Tiburón island and south of Punta San Francisquito. There is no evidence of strong tidal pumping between the Northern Gulf and the Southern Gulf along Ballenas Channel.

South of the archipelago (Fig. 2b), there is a relatively strong southward coastal flow ($\mathbf{u}_e \sim 2$ cm s^{-1}), from Punta San Francisquito to San Marcos Island. Further south, there are mesoscale eddies in the vicinity of Santa Catalina, Carmen and Cerralvo islands.

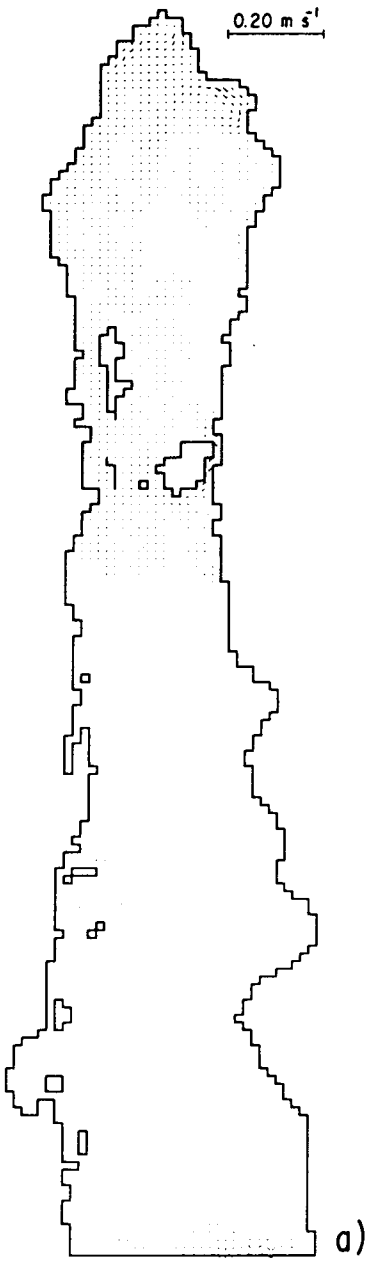

(Fig. 2a).

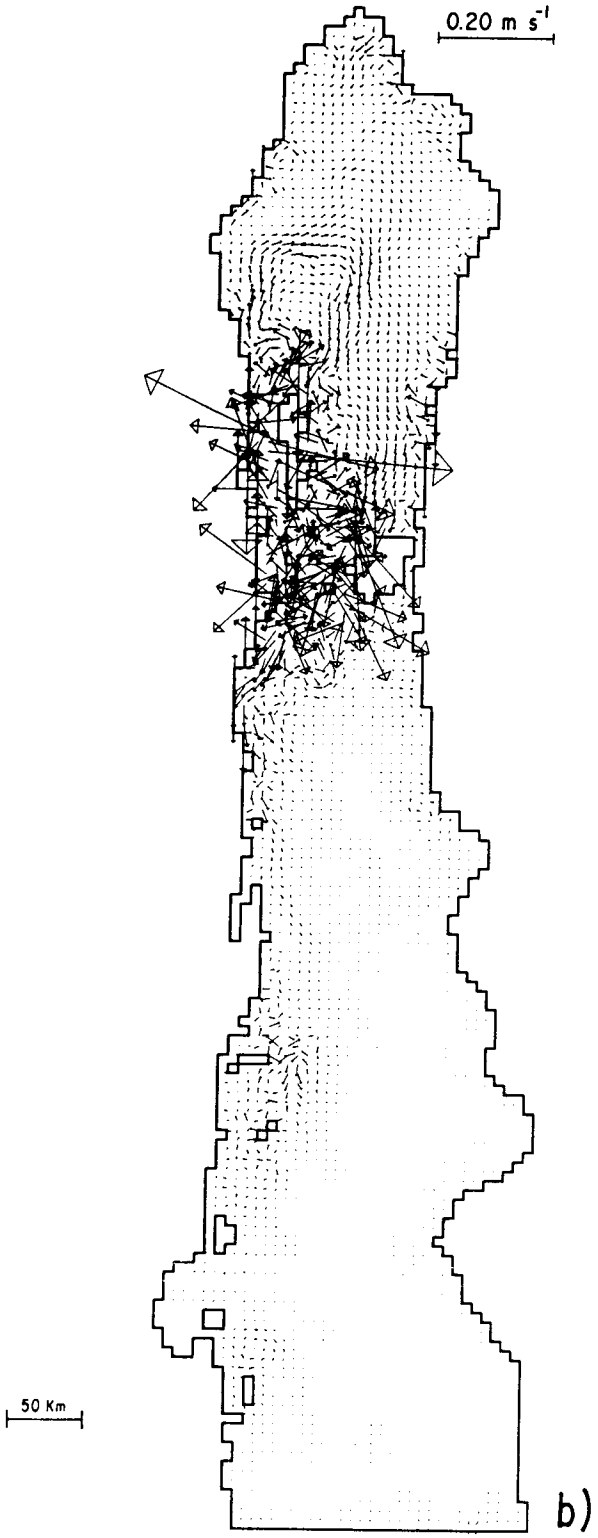

(Fig. 2b).

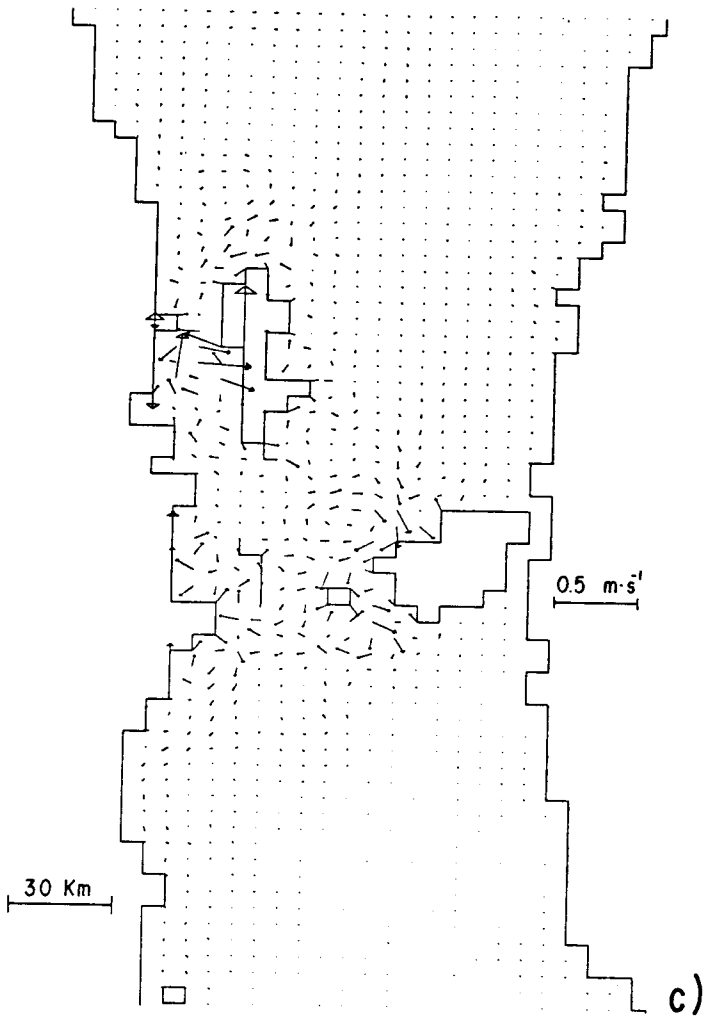

Fig. 2. Eulerian residual flow $\mathbf{u}_e$ in the Gulf of California: (a) with the linearized model (neglecting the advection term), (b) with the nonlinear model, (c) also with the nonlinear model, but in a different scale in order to better show the circulation pattern in the archipelago.

Huthnance (1973, 1981) has shown that tidal residuals are due to the friction and Coriolis terms, and that when the Coriolis term is dominant, the flow tends to follow the h/f contours; thus when f is constant the flow is along the isobaths. Therefore, in the Upper Gulf the frictional term dominates the balance against the pressure gradient, while in the deeper parts of the Northern Gulf the pressure gradient is balanced mainly by Coriolis force; this is in agreement with the discussion of the relative importance of the terms of the dynamical equations for the tidal means in the Northern Gulf made by Marinone (1997). Since the tidal excursion ($\sim$ 3 km in the Northern Gulf) is smaller than the grid size (6.6 km), therefore the residual flow generated by topographic structures of a size comparable to the tidal excursion is not resolved (Zimmerman, 1980; Robinson, 1983).

a. Comparison with other models

Comparison between the tidal-induced residual currents predicted by our model and those estimated from current meter data, presents a series of difficulties. In the first place, the mag-

nitude of the predicted flow is of the order of 1 to 2 cm s^{-1}, which is approximately the limit accuracy of the best current measuring system. On the other hand direct current measurements include contributions of mechanisms such as wind stress and sea level differences, therefore it is nearly impossible to obtain measurements where these mechanisms are not in operation.

Due to this difficulty and in order to have an assessment of the validity of the model's results we compare our distributions against those predicted by three different 2D models; making emphasis on the order of magnitude of the currents and the main flow pattern. These models are those of Quirós *et al.* (1992), Carbajal (1993) and Marinone (1997).

Although there are discrepancies between the models regarding the direction of the flows, they all agree that the speed of the currents is about 1 or 2 cm s^{-1}.

The best qualitative consistency was obtained between our results and those of Marinone (1997), the spatial distributions of both models show: i) weak residual flows in the Southern Gulf and ii) stronger currents on the archipelago area and on the shallow Northern Gulf.

Quirós *et al.* (1992) spatial distribution although similar to our distribution, that is, with weaker currents in the Southern Gulf and stronger currents near the archipelago and in the Northern Gulf, presents important difference. In Ballenas Channel they indicates no flow while our model predicts maximum velocities; in fact they have maximum velocities near the head of the Gulf. In addition, they do not obtain the anticyclonic gyre over Delfín Basin shown in Figure 2b is not obtained by them.

The discrepancies between our results and those of Quirós *et al.* (1992) could be associated to the 14 km mesh used in their model, which could by be too large to define the topography of the archipelago and the depth gradients in Delfín basin. The complicated pattern predicted by our model in the archipelago (Fig. 2c), suggest that an even finer grid may be necessary. The possibility that these discrepancies may be due to the different mesh size used in the models has been investigated by G. Marinone (*personal communication*). Running a 2D model with a grid and bathymetry used here and with the grid and bathymetry used by Quirós *et al.* (1992), a pattern similar to the one found here was obtained in both cases.

Carbajal (1993) has run 2D and 3D barotropic models of the M2 tide in the gulf. His 2D model has a 6' mesh (~9.5 km in the Northern Gulf), and the currents pattern (his Fig. 4.11), also have significant differences with Figure 2b. Although there appears to be anticyclonic circulation around Delfín basin, the circulation in the Upper Gulf is, overall, stronger and in the opposite sense to that obtained here and by Marinone (1997). Also, he finds a consistent NW flow along Ballenas Channel. The 3D model has a 3' grid, or ~5 km in the Northern Gulf, where the flow (his Fig. 4.25) in the top layer (0-10 m) is across the gulf, toward the peninsula. Unfortunately, the vertically integrated tidal is not shown by Carbajal (1993).

In general the differences between our results and those of Quirós *et al.* (1992) and Carbajal (1993) must be associated to the spatially variable coefficients of bottom friction (C_d) and eddy viscosity (K_h) used in their models. In both cases these parameters were allow to vary in order to achieve an empirical fit between the modeled tides and the observations.

Quirós *et al.* (1992) used a spatially variable bottom friction coefficient of the form:

$$C_d = (1/32)[1/(\ln(19.8h/(\phi))^2] :$$

which is function of the bottom sediments diameter (ϕ) and the water depth (h). Due to the lack of sediments data a series of trials were performed with different values of ϕ in order to obtain the best fit with the observation. A value of $\phi = 10$ was chosen. With this C_d relation, for the depth variations of the gulf, its value differ by one order of magnitude (from 10 m to

~3,000 m with C_d values are $\sim 3.5 \times 10^{-3}$ and $\sim 0.40 \times 10^{-3}$ respectively). In this context, Marinone (1997) indicated that for the case of his model, in which C_d was assumed spatially constant, significant differences among runs are obtained if C_d varies by more than 30 %. This author also found that for variations of C_d inside the range of 30 % the spatial structure of the currents is preserved and their magnitude increased as C_d decreases. It is evident that a further complication arises when C_d values differ by one order of magnitude, in distances of few kilometers for a single run of the model. On the other hand, Carbajal (1993) considered a variable eddy diffusion coefficient of the form:

$$K_h = A\Delta l(h);$$

here; A is a constant (2×10^{-4}), Δl is the grid size, and h the water depth. Eddy diffusion values obtained from this relation for areas where the bottom slope is pronounced as, is the case of the vicinity of the archipelago and the Southern Gulf basins, can presents variations of $K_h > 10^2$ m^2 s^{-1} in distances of ~10 km. Although in general the diffusive term due to lateral eddy viscosity, in numerical models acts to redistribute vorticity such that steep gradients are smoothed out; in this case the spatial variation of K_h generates vorticity. This could explain at least partially the presence of relatively strong residual flows in the vicinity of the islands and in the Southern Gulf and which was not predicted in the models compared here. Although in general the use of eddy viscosity artificially large is common problem in numerical models, so that sufficient energy dissipation can occur on scales resolvable by the numerical scheme. Nevertheless this is no guarantee that this procedure will remove energy in a realistic way and a major problem of numerical modeling is to found schemes that will remove energy realistically.

4. Wind-induced circulation

Wind is highly polarized along the gulf (Badan-Dangon *et al.*, 1991b), with strong northwesterlies in winter and weak southeasterlies in summer. Winter winds records has a significant feature; the occurrence of intense wind events, with speeds ~10 m s^{-1}. Strong northwesterlies with a mean duration of 2 to 3 days has been reported in San Felipe (Reyes-Hernández *et al.*, 1997), and in meteorological data reports of six islands and coastal locations in the Gulf of California (Merrifield *et al.*, 1987). In Tortugas Island winter winds speeds up to 15 m s^{-1} are reported. Also in the wind records presented in the next section this strong winter events are evident.

The wind driven circulation was simulated, including on the working model of the M_2 tide the wind stress term (τ_w,) spatially constant. Only the NW and SE wind directions were simulated assuming that, the wind stress τ_w was related to the wind W_{10}, at a height of 10 m, by the relation given by equation (4). For the simulations presented here it was considered a wind speed of 10 m s^{-1}, which with a value of $C_{10} = 1.3 \times 10^{-3}$ gives a wind stress of ~0.016 Pa. For simulations with smaller wind stress values (7.5 m s^{-1} (~0.008 Pa) and 5.0 m s^{-1} (~0.0034 Pa)), the current patterns were similar, with reduced current speed and are not presented here.

The residual flows and sea levels due to wind forcing were determined, as suggested by Pingree and Griffiths (1980), assuming a steady wind stress acting on the modeled area. The resulting velocities and elevations were averaged over a tidal cycle using equation (5) and then subtracting the tidal residuals.

a. Results

The wind driven circulation for NW and SE wind directions and the corresponding sea level elevations are shown in Figure 3. For both wind directions the current patterns are almost the same, but with the current direction reversed (Figs. 3a and 3c). The overall circulation is anticyclonic for NW wind and cyclonic for SE wind. In both cases the maximum velocity (up to 15 cm s^{-1}) is predicted south of the archipelago, in a jet along the entire length of the mainland continental shelf, in depths less than 200 m. By contrast, the return flow off the peninsula coast is weaker ($\sim$5 cm s^{-1}) and less organized. The large horizontal shear apparent in the coastal jet may be important in the generation of the upwelling filaments that separate from the capes of the mainland side of the gulf (Badan-Dangon *et al.*, 1985; Navarro-Olache, 1989). The jet is associated to a surface tilt across the mainland shelf (Fig. 3b). It seems that the difference in continental shelf width is responsible for this asymmetric response of the coastal currents to the wind.

As the model is barotropic it is evident that winter conditions are expected to be more realistically simulated henceforth, only the effects of NW winds, typical of the winter, will be described (Figs. 3a and 3b), the results for SE wind case (Fig. 3c) differing in having the opposite sign.

In the Northern Gulf, the main feature is an anticyclonic jet exceeding 5 cm s^{-1} which in some places flows in direction opposite to that of the wind; it starts in the west of Delfín Basin, follows the maximum bottom slope (depth contours between $\sim$100 m and $\sim$150 m) as far as the northern end of Wagner Basin, and then veers and fans out, thence following the mainland coast off Bahía Adair and Bahía San Jorge, all the way to Tiburón island. This return flow occurs in depths less than 40 m, and it is here that the maximum current speed ($<$ 10 cm s^{-1}) in the Northern Gulf occurs. Between the jet and the peninsula, an elongated cyclonic circulation is established, and another cyclonic gyre is formed on the peninsula side of the Upper Gulf. Therefore the coastal currents are toward the mouth on both sides of the Northern Gulf: from the Upper Gulf to Bahía San Luis Gonzaga in the peninsula coast, and as far as Tiburón island in the mainland side.

The wind does not drive a continuous exchange between the Upper and the Southern Gulf across the channels between the islands. In Ballenas Channel, the only organized flow is found close to the peninsula coast, and it is directed toward the SE. South of Angel de la Guarda island there is a minimum in current speeds, again without a clear pattern. Maximum currents ($\sim$10 cm s^{-1}) are found over the San Lorenzo sill; these currents appear to drive a flow towards the Upper Gulf in the San Lorenzo and San Esteban channels. By contrast, the flow through the Tiburón channel is directed towards the Southern Gulf. The lack of a clear wind-driven water exchange between the Northern Gulf and the Southern Gulf may affect the renewal of the water in the NGC and may be relevant for the interchange of passive tracers, like plankton, nutrients, sediments, etc.

Immediately past the islands, there is a clear anticyclonic circulation that follows the bathymetry, in a fashion very similar to that found in the Northern Gulf: from off Santa Rosalía to Punta San Francisquito, the flow is toward the Upper Gulf (against the wind direction), then it veers following the bathymetry south of the islands, then veers again south of Tiburón island to join the windward coastal jet described previously. The current speed is $\leq$ 5 cm s^{-1} off Baja California and reaches speeds up to 10 cm s^{-1} as it veers south of Tiburón island.

The distributions of the surface elevation corresponding to the wind-induced currents (Fig. 3b) shows surface slopes over the continental shelf of the Northern Gulf and the east coast of the

Southern Gulf where the continental shelf is wider than that along the peninsula. This indicates the important role of bottom depth variations on the distribution of wind-induced currents and in general on the dynamics of the Gulf.

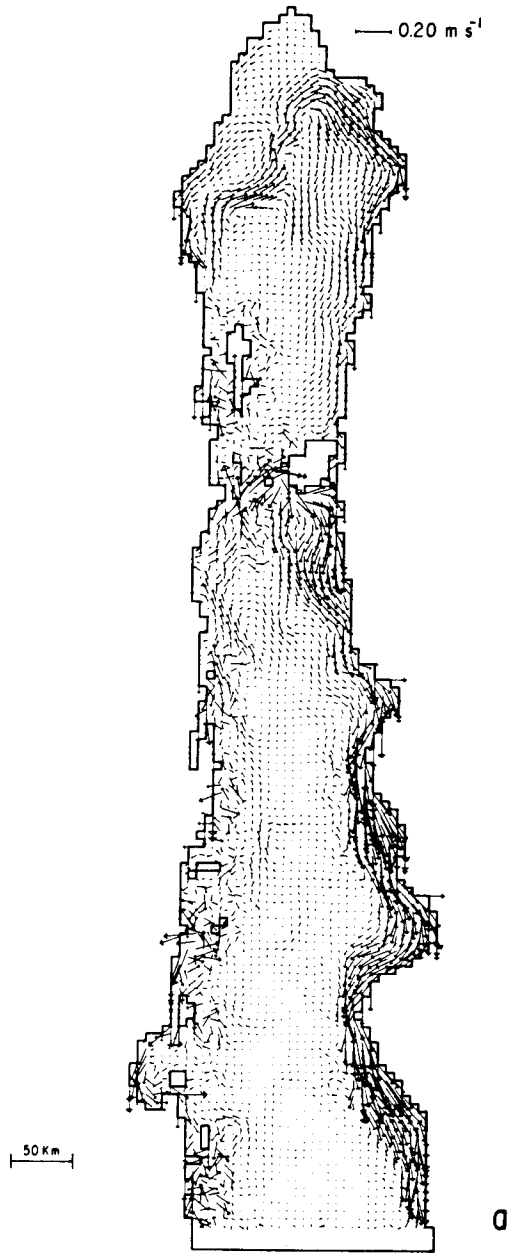

Fig. 3a

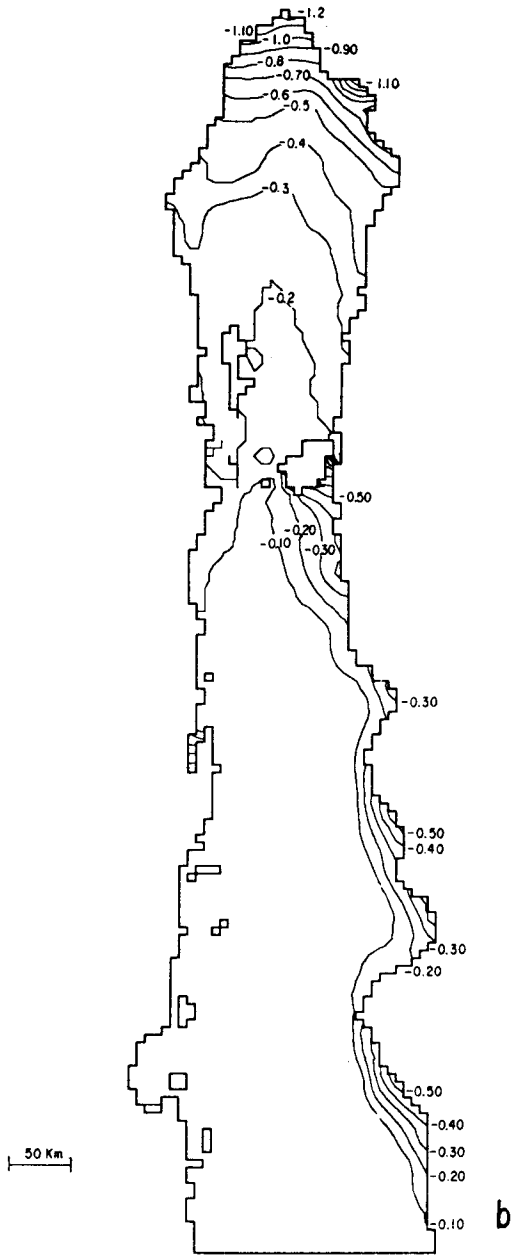

Fig. 3b

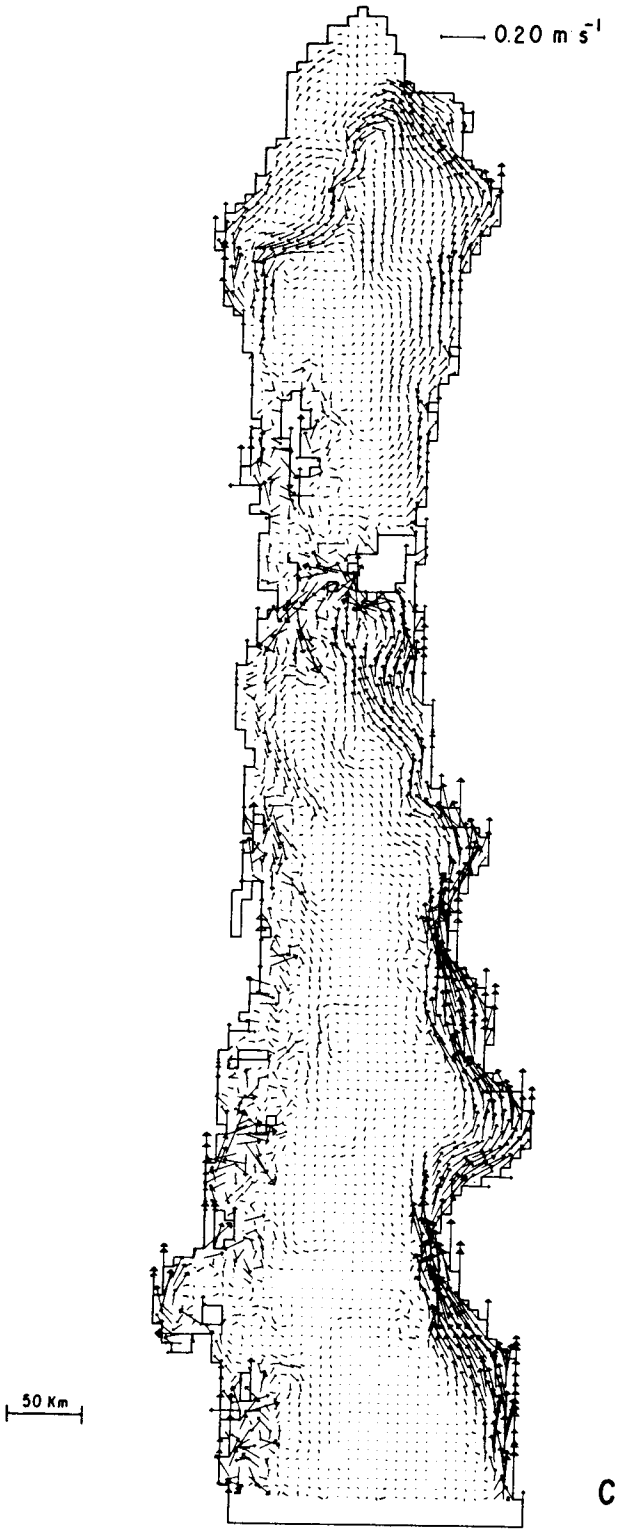

Fig. 3. Wind driven residual resulting from a uniform wind stress, $\tau_w = 0.016$ Pa: (a) NW wind, (b) The sea level in cm, corresponding to the NW wind residuals (c) SE wind.

In the Northern Gulf the bathymetry presents significant variations in the direction perpendicular to the wind, while in the Southern Gulf, there are significant depth variations between near shore and offshore. Under these conditions it is expected that wind stress will set up large pressure gradients in the shallow waters which cannot be maintained in the deeper offshore areas, therefore the circulation pattern will present stronger flow in the wind direction near shore and reduced return flow in deeper waters. This effect of the bathymetry on wind-induced circulation has been studied analytically (Csanady, 1984) and predicted by numerical modeling of semi-enclosed sea regions (Pingree and Griffiths, 1980; Argote *et al.*, 1991).

The component of the wind along the coast could generate coastally trapped waves. In the presence of shelf topography (even without stratification) wind forcing generates continental shelf waves that propagate along the boundary. On the other hand in the presence of stratification and constant depth, free waves propagate along the coast in the form of an internal Kelvin wave. In real conditions hybrid waves with characteristics of both, Kelvin an shelf waves called coastally trapped waves, exist (Gill, 1982). Evidence of this hybrid form of waves propagating along the east coast of the gulf, has been indicated by Christensen *et al.* (1983), based on sea level data. These authors identify the presence of hybrid waves with a phase speed of 4 ms^{-1}, an offshore scale < 200 km and, a volume transport of near zero. They estimate for the internal Kelvin wave a phase speed of 2.1 m s^{-1} and an offshore scale of 50 km, while for the barotropic shelf wave a phase of 2.3 m s^{-1} and an offshore scale of 60 km. The authors could not identify the origin of these waves. Although the analysis of these waves is out of the reach of this work, it is important to notice that the offshore scale of the barotropic wave estimated by Christensen *et al.* (1983) is consistent with the length of the coastal strip, along the east coast of the gulf, were sea surface elevation (Fig. 3b) showed a marked response to wind forcing. It is evident that the response of the coastal boundary of the gulf to the wind forcing poses a great number of questions that requires further investigation.

b. Comparison with other models

The wind driven circulation in the Gulf of California has been modeled by Dressler (1981), using a 2D model with a 14 km grid, and by Carbajal (1993), using the homogeneous 3D model mentioned above (3' grid). They both used a 5 m s^{-1} NW wind. Despite the low-resolution mesh, Dressler (1981) obtained an anticyclonic gyre in the Northern Gulf.

The depth-averaged circulation obtained by Carbajal (1993) (his Fig. 5.5) is very similar to that obtained here (Fig. 3a), including the anticyclonic flow in the Northern Gulf, and the coastal jet along the entire mainland coast in the Southern Gulf. Important differences are that this author obtained a well-organized return flow (toward the Upper Gulf) over most of the width of the Southern Gulf, which continues to the Northern Gulf across the sills, on both sides of Angel de la Guarda island. He also obtained a windward flow along the coast of the Peninsula (which is also present in Figure 3a), although not continuously; it is especially clear in and to the NW of Bahía de La Paz.

Beier's (1997) two-layer linear baroclinic model also predicts anticyclonic surface circulation in winter and cyclonic in summer. The strongest currents occur at the intersection of the interface with the bottom (70 m). Much higher surface velocities are obtained by this baroclinic model than by any of the barotropic models, but the flow does contain important a barotropic component in the Northern Gulf (Beier, 1997).

5. The observations

Although some current meter observations have been made before in the Gulf of California (Merrifield and Winant, 1989; Bray, 1988b; Badan-Dangon *et al.*, 1991a; Alvarez-Sánchez *et al.*, 1993; Argote *et al.*, 1995; Salas-Pérez, 1996), no coherent description of the circulation can be obtained from them, due to the limitations like lack of simultaneity, shortness of duration, etc. In order to overcome these limitations, simultaneous wind and current observations were carried out in the Northern Gulf in December 1994 and January 1995, at the sites and times listed in Table 1 and marked in Figure 1. The observations were made in the Northern Gulf during winter so, that conditions as close to barotropic as possible be encountered: the surface mixed layer exceeds 60 m and sometimes reaches 100 m (Martínez-Sepúlveda, 1994), and the coastal well-mixed area extends to the 60 m isobath (Organista-Sandoval, 1987; Argote *et al.*, 1995).

Table 1. Location of Current Meters and Meteorological Stations

Location	Latitude N	Longitude W	Instrument	Bottom Depth (m)	Meter Depth (m)	Start Date (m/d/y)	Record Length (days)
MetBuoy	31° 03.00'	114° 51.8'	Minimet	200		12/06/94	46
Mary-I	30° 21.80'	114° 11.0'	G.O. 420	150	21	11/28/94	14
			G.O. 481		60		
			G.O. 490		120		
Mary-II	30° 22.50'	114° 11.4'	G.O. 420	150	21	12/13/94	40
			G.O. 481		60		
			G.O. 490		120		
Lilia	31° 11.30'	113° 57.9'	Endeco-048	52	19	11/27/94	9
			G.O. 617		29		
Rosalba	30° 42.50'	114° 14.9'	Endeco-048	95	28	12/07/94	51
			G.O. 617		85		
Tere	30° 03.93'	114° 16.5'	G.O. 606	200	38	11/30/94	69
			G.O. 489		120		
Paty	30° 23.31'	113° 43.3'	G.O. 424	150	25	11/28/94	27
			G.O. 421		120		

The sites were selected on the basis of the main features of the simulated flows under NW winds. Unfortunately, no instruments can be installed for long in water less than 100 m during winter due to the presence of the shrimp's fleet.

a. Instruments

A Minimet meteorological buoy was used equipped with a Young Model 05103 wind monitor, a NAVICO HS8000 heading sensor and a ZENO-800 logging system. The accuracy of the wind measurements is $+0.2$ m s^{-1} and $\pm 5°$. The current meters were General Oceanics Niskin current meters (inclinometer type) Model 6011 MkII, with accuracy of $+0.01$ m s^{-1} and $\pm 2°$; also used was one Endeco Type 174 SSM current meter, accurate to $+0.02$ m s^{-1} and $\pm 5°$. They were deployed in acoustically released I-type moorings with the uppermost flotation unit at least 15 m under the surface.

b. Data processing

After checking the operation of the instruments' clocks and correcting any drifts, the raw time series were smoothed, sampled once an hour, and then low-passed with Godin's (1988) filter. This filter eliminates diurnal and semidiurnal variations, including inertial oscillations. The low-passed time series are shown in Figures 4 to 9.

c. Results

There were several days with NW winds prior to the deployment of the meteorological buoy on December 6; the NW winds lasted until December 24 (Fig. 4). The low-passed wind velocity shows speeds up to 10 m s^{-1}. The current meter data collected during this NW wind event will be used to make a qualitative comparison with the results of the numerical model run with NW wind.

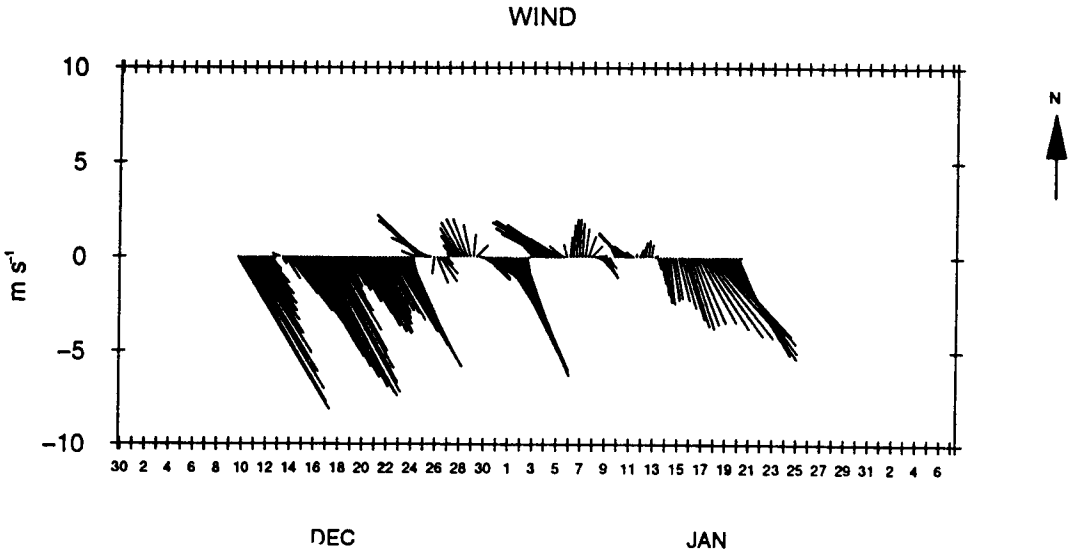

Fig. 4. Low-passed wind vectors at the Meteorological Buoy.

During the NW wind event, the low-passed near-surface currents show a behavior clearly dependent on their position with respect to the gulf axis. Moorings TERE (Fig. 5) and MARY (Fig. 6), which were located on the peninsula side (Fig. 1), show flow going in a N or NE direction, respectively; that is, in a direction opposite to that of the wind. Meanwhile LILIA (Fig. 7) and PATY (Fig. 8), which were in the mainland side of the gulf, show currents roughly following the direction of the wind. These data clearly show a pattern of anticyclonic surface circulation in the Northern Gulf during NW winds, which breaks down when the wind abates.

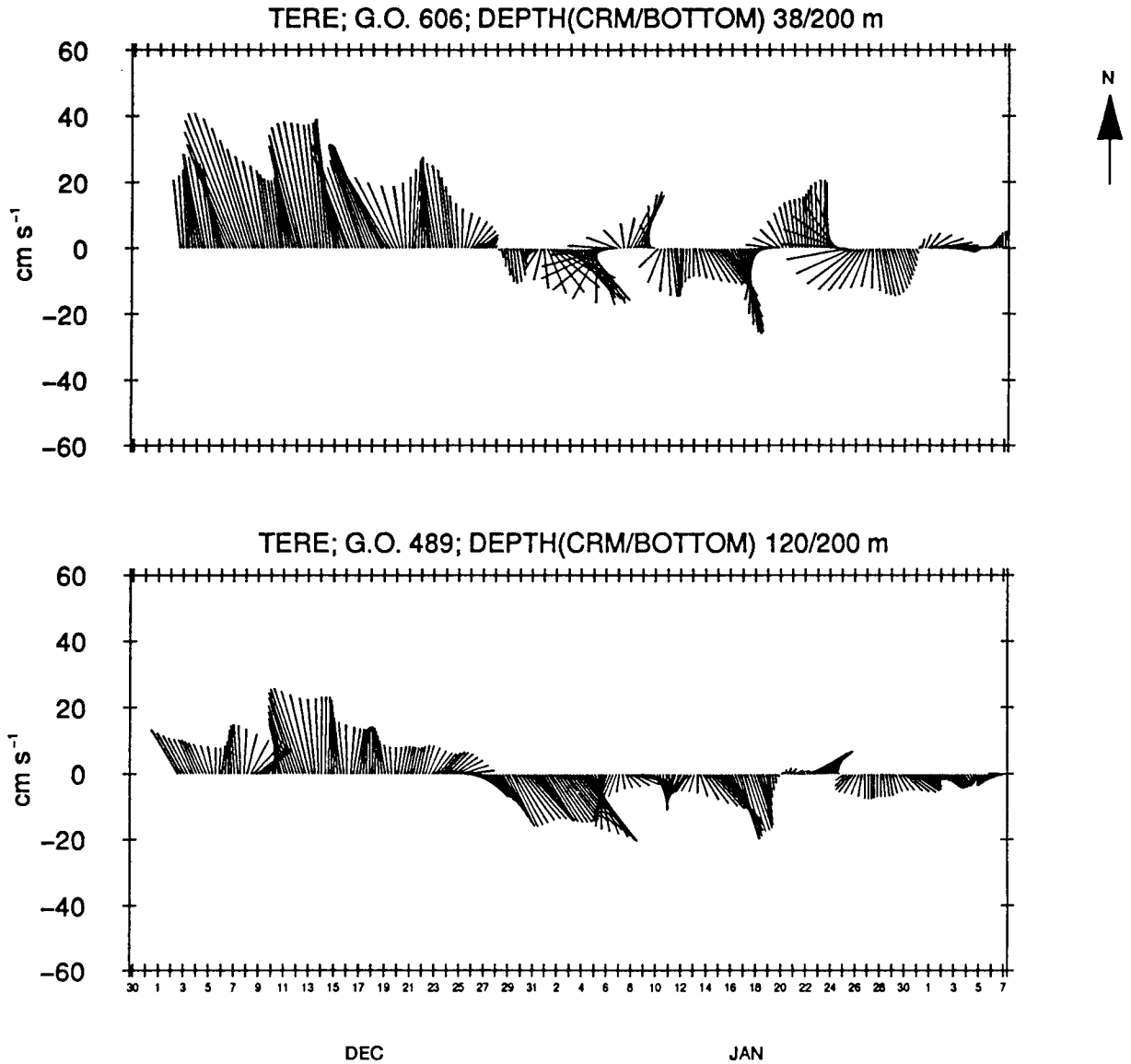

Fig. 5. Low-passed current vector time series at mooring TERE. The headings list the mooring name (Table 2), the trade-mark and serial number of the current meter (G. O. = General Oceanics), the depth of the instrument in the water column and the bottom depth. Position is given in Table 2 and Fig. 1.

Not all the data fall into the simple anticyclonic pattern, of course; mooring ROSALBA (Fig. 9) shows no well-defined surface speed or direction during the NW wind, and the deepest current meter in mooring MARY (Fig. 6c) strongly suggests the strongest baroclinicity. Although during winter, wind mixing and lower or negative surface heat flux give rise to vertically mixed conditions in the upper layer of ~100 m, in deeper areas stratification prevails, although this is weaker in relation to summer conditions (Argote *et al.*, 1995). Therefore the baroclinic conditions shown by the moorings and not considered in the model must be considered to conciliate the discrepancies between the observed conditions and those predicted by the model.

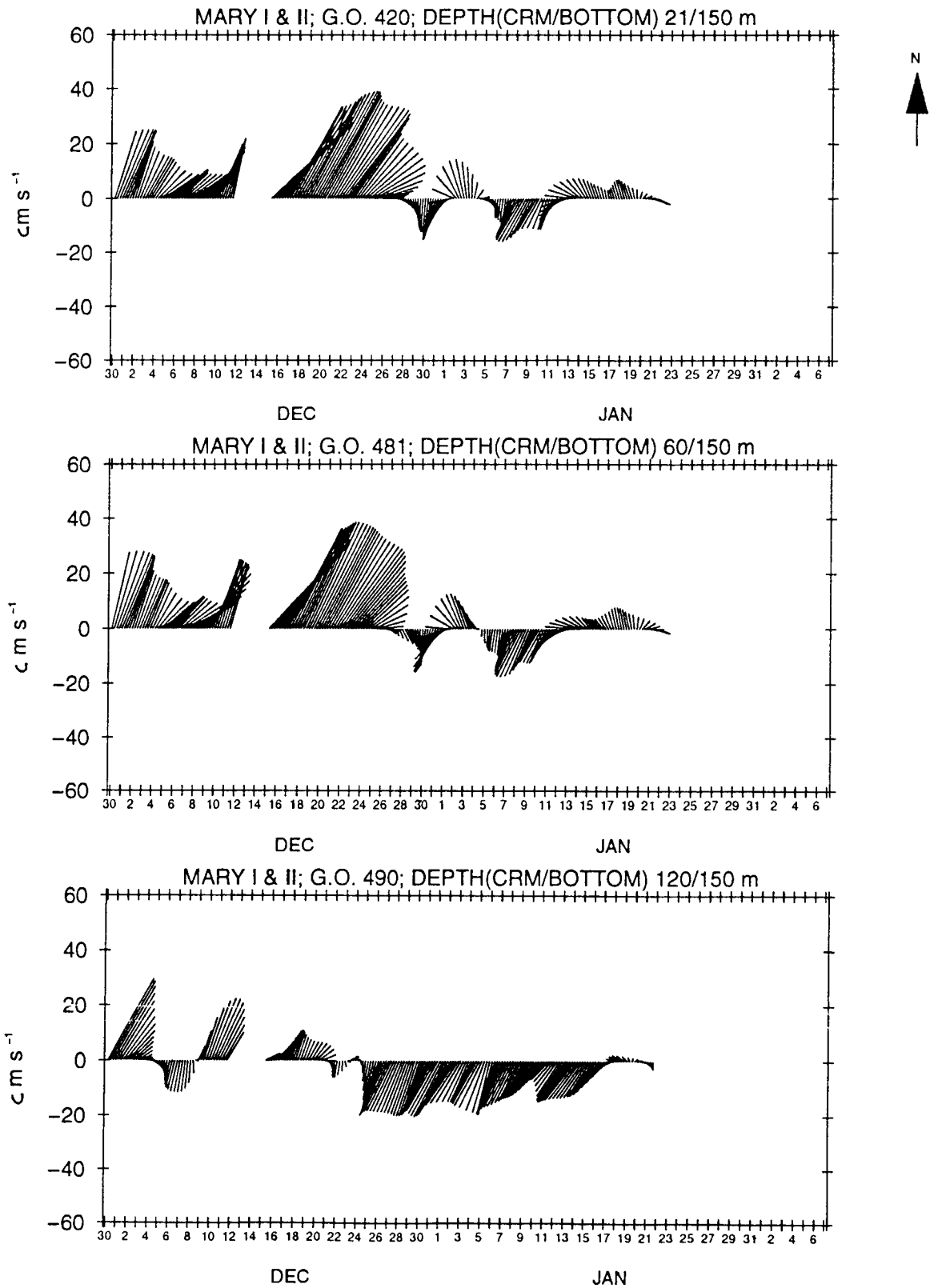

Fig. 6. Same as Fig. 5, but for moorings Mary-I and Mary-II.

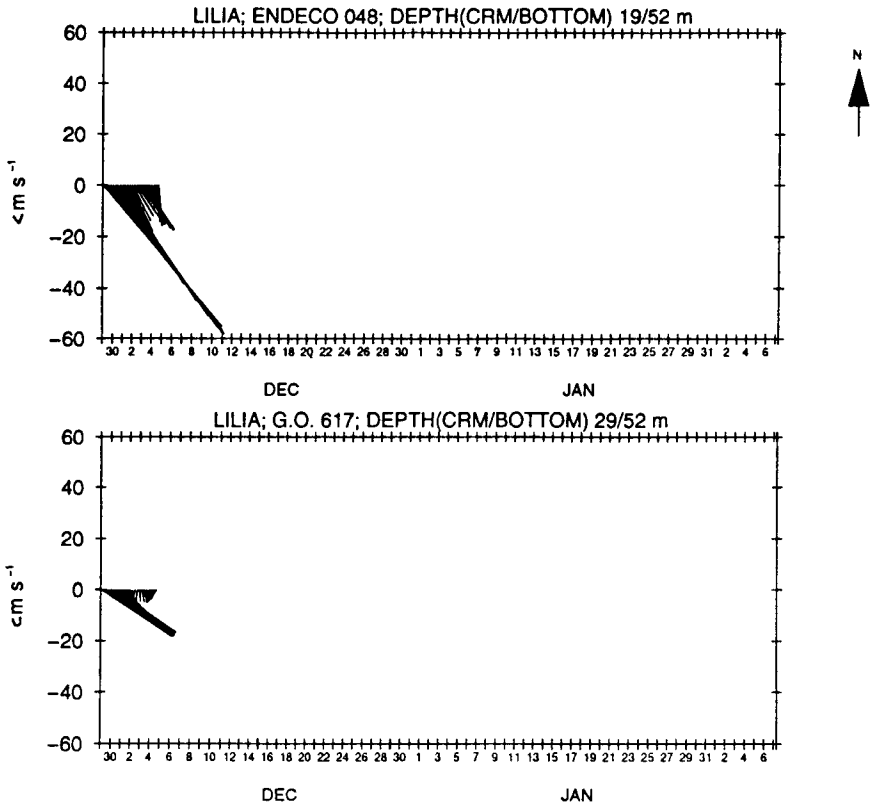

Fig. 7. Same as Fig. 5, but for mooring LILIA.

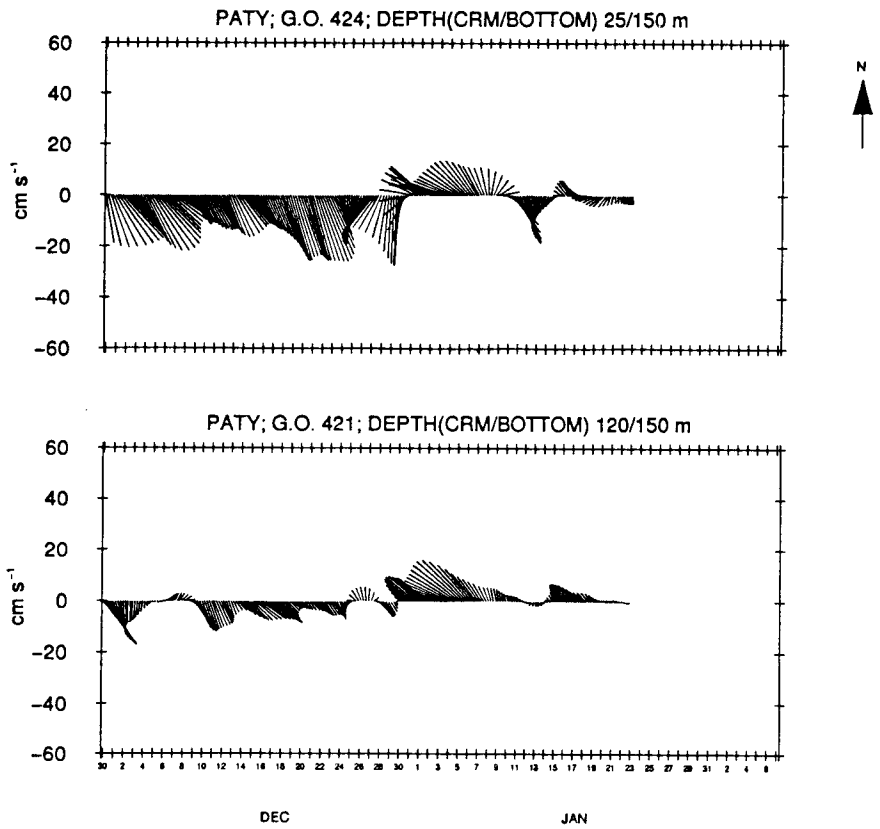

Fig. 8. Same as Fig. 5, but for mooring PATY.

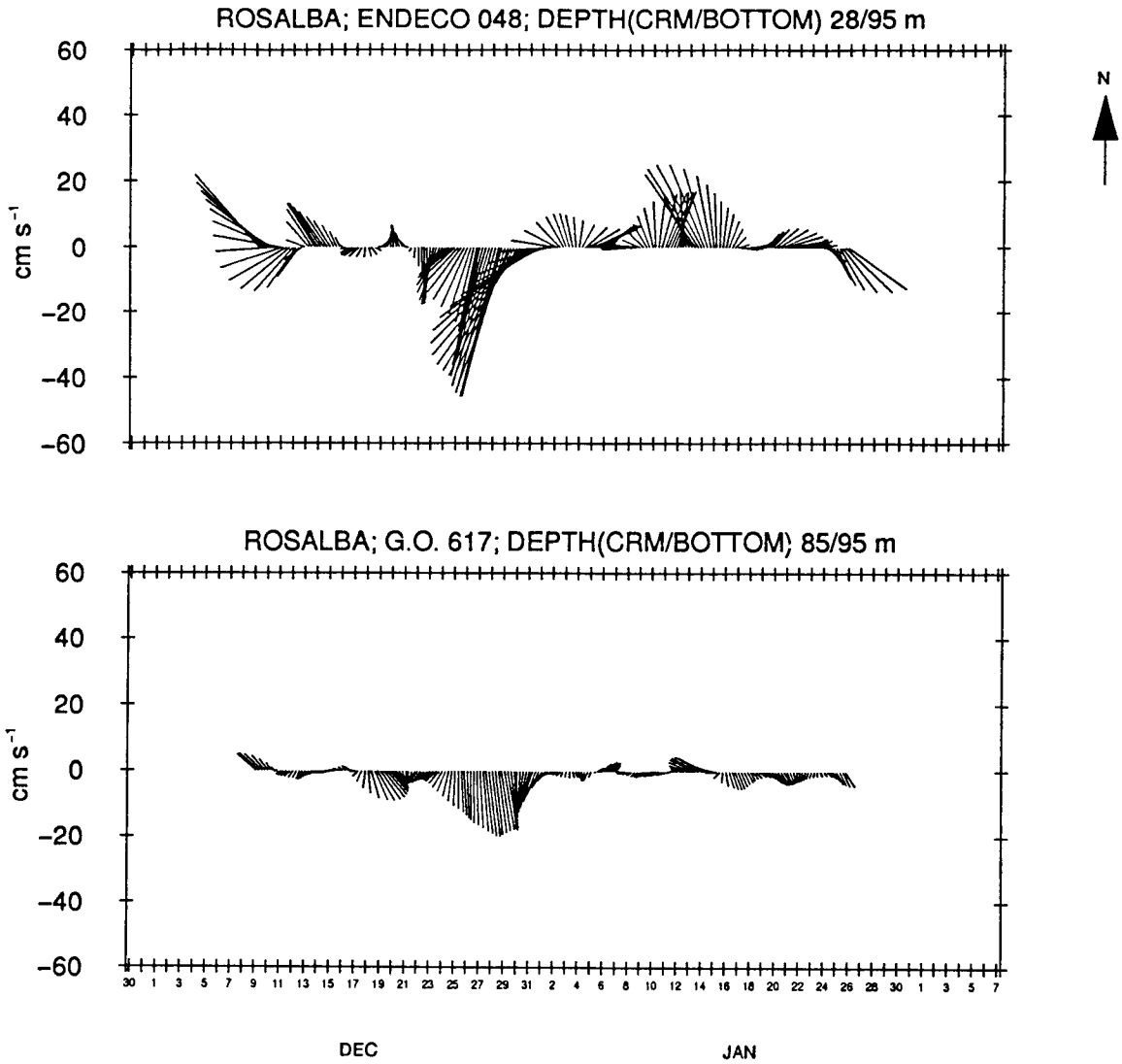

Fig. 9. Same as Fig. 5, but for mooring ROSALBA.

d. Comparison between the model and the observations

The comparison of the simulated wind-driven currents against the observed currents described before is summarized in Figure 10, which is a zoom-in of the model results for NW wind in the Northern Gulf, with the mean current velocities observed with the current meters overlaid with thicker arrows. The low-passed data from the upper two current meters were vector-averaged for the period November 30 to December 26 of 1994, and then averaged in the vertical. There is qualitative agreement on several important features, but the measured currents are clearly stronger. This may be explained by the fact that conditions were not completely barotropic, and to the fact that the wind field was assumed stationary and homogeneous, which is a simplification of the real conditions as it is shown in Figure 4.

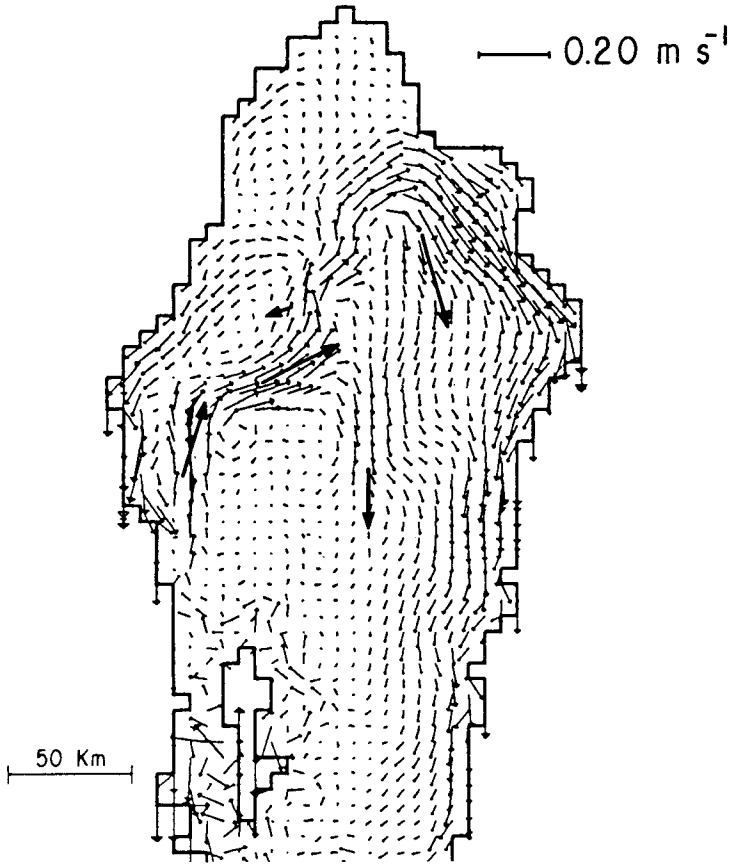

Fig. 10. Comparison between, simulated wind driven currents resulting from a uniform NW wind stress of 0.016 Pa and those estimated form current meter rigs under NW wind.

The features that are in agreement are: (a) the N or NE flow in the rim (maximum bottom slope) of Delfín Basin (moorings TERE and MARY, Figs. 5 and 6); (b) the flow toward the S or SE on the mainland side (moorings LILIA and PATY, Figs. 7 and 8). Mooring ROSALBA (Fig. 9) seems to have been located near the place where the jet along the bottom slope of Delfín and Wagner Basins bifurcates, to form the elongated cyclonic gyre between the slope and the peninsula.

Observations made with Lagrangian drifters (Lavín *et al.*, 1997) show that in winter there is an anticyclonic gyre whose position coincides with that predicted by the model with NW winds. Moreover the gyre is mostly barotropic, since observed currents are much stronger than geostrophic calculations made from a concurrent CTD survey. Therefore at least for the Northern Gulf in winter, the barotropic wind-induced currents are quite significant, and in some agreement with the model results.

The agreement between the model and the observations can only be claimed to be qualitative, and that for the Northern Gulf in winter, but the evidence provides confidence in the predicted general pattern of wind induced currents. Of course, the wind stress is quite variable, so that a steady wind as that used here can only be regarded as an approximation. The main limitation of the model is that stratification is found almost everywhere in the gulf in summer and in

water over 100 m deep in winter (Martínez-Sepúlveda, 1994). The tidal-mixing fronts described by Argote *et al.* (1995) probably induce baroclinic currents, as do the fronts associated to coastal upwelling. In areas near shelf sea fronts direct current measurements indicate flows with magnitudes up to ~30 cm s^{-1} which are not always parallel to the mean front orientation. The complex circulation patterns with flows perpendicular to the fronts seems to be due to the presence of eddies generated by baroclinic instabilities. These subjects are currently under study, both by numerical and observational studies.

6. Conclusions

A vertically integrated non-linear numerical model was used to analyze the effect of two forcing mechanisms of the mean barotropic circulation in the Gulf of California: topographic rectification of the M_2 tidal currents, and wind stress.

The interaction of the M_2 tidal currents with the bathymetry is important in the Northern Gulf and in the region between the islands. The tidal-induced currents in Ballenas channel are about 5 cm s^{-1}, but they are disorganized. In the Northern Gulf, an anticyclonic circulation (~2.5 cm s^{-1}) is established around the edge of Delfín Basin, and a smaller and slower cyclonic gyre is formed in Adair Bay. The circulation along the isobaths in a bottom slope is due to the advective terms of the equations; by contrast, the currents at the Upper Gulf are due to the quadratic frictional term. No tidal pumping between the Northern Gulf and the Southern Gulf seems to be produced in the channels and sills. In general, the tidal-induced currents are of O(1 cm s^{-1}).

For a NW wind (winter conditions), the main features of the predicted circulation are (for SE winds, the direction of flow is reversed):

(i) In the Northern Gulf, an anticyclonic circulation pattern over the edge of Delfín and Wagner Basins, which continues along the mainland coast as far as Tiburón island. In the Upper Gulf, two cyclonic gyres are formed on the peninsula side.

(ii) In the Southern Gulf, a coastal jet (speed up to 15 cm s^{-1}) flowing in the wind direction is predicted along the continental shelf of the mainland. This asymmetry seems to be due to the different width of the continental shelf in the two sides of the Gulf.

(iii) There is a return flow in the Southern Gulf, but it is much weaker and unorganized, except between Santa Rosalía and the islands, where an anticyclonic pattern similar to that of the Northern Gulf is established around the NW edge of Guaymas Basin.

(iv) No clear water exchange between the Northern Gulf and the Southern Gulf seems to be established by the wind. In the two channels separated by San Lorenzo Island, a flow towards the Northern Gulf is established, while between San Esteban island and Tiburón island the flow is toward the Southern Gulf.

The current meter observations, taken in the Northern Gulf during a strong winter NW wind event lasting about two weeks, support the formation of an anticyclonic circulation in the Northern Gulf during NW winds. However, the observed currents are stronger than the model prediction. The barotropic anticyclonic circulation predicted by the model in the Northern Gulf is also in agreement with drifter observations.

(v) In the Northern Gulf, during winter the wind forcing has a more pronounced effect on the mean circulation than tidal forcing. Wind driven currents reach speeds > 5 cm s^{-1} over wide areas than those where tidal-induced flow reach maximum speeds (~2.5 cm s^{-1}).

On the Southern Gulf tidal-induced mean flow is in general weak compared with the stronger mean flow induced by the wind.

The main limitation of this study is the use of a barotropic model; baroclinicity is certain to be always important in the Southern Gulf and during the summer in the Northern Gulf. Nonetheless, there is evidence that barotropic currents are a significant component of the flow field. Further studies, both numerical and observational, which take stratification into consideration, are currently underway.

Acknowledgements

This study was funded by the Government of Mexico through CICESE, and through CONACYT contracts 4929-T (M.L.A.) and 3209-T (M.F.L.). J. R. Hunter kindly provided the numerical model. The model graphs are by F. Plaza, and finished artwork is by J. M. Domínguez. Current meter data processed by E. Palacios and J. García. Technical support by Carolina Morales and Secretarial support by Felicitas Velasco. We also thank anonymous referees for their helpful comments in an earlier version.

REFERENCES

Alvarez-Sánchez, L. G., A. Badan-Dangon and J. M. Robles, 1984. Lagrangian Observations of near-surface currents in Canal de Ballenas: California Cooperative Oceanic Fisheries Investigations (CalCOFI), Report 25, 8 pp.

Alvarez-Sánchez, L. G., V. Godínez, M. F. Lavín y S. Sánchez, 1993. Patrones de turbidez y corrientes en la Bahía de San Felipe, al NW del Golfo de California. Comunicaciones Académicas CICESE, Ensenada, México. CTOFT-9304, 48 pp.

Argote, M. L., F. J. Medina and A. Amador, 1991. Wind-induced circulation in Todos Santos bay, B. C., Mexico. *Atmósfera*, **4**, pp. 101-115.

Argote, M. L, A. Amador, M. F. Lavín and J. H. Hunter, 1995. Tidal dissipation and stratification in the Gulf of California. *Jour. of Geophys. Res.*, **100**, pp. 16103-16118.

Badan-Dangon, A., C. J. Koblinski, and T. Baumgartner, 1985. Spring and summer in the Gulf of California: Observations of surface thermal patterns, *Oceanológica Acta*, **8**, 13.

Badan-Dangon, A., M. Hendershott and M. F. Lavín, 1991a. Underway Doppler current profiles in the Gulf of California, *EOS*, **72**, 209, pp. 217-218.

Badan-Dangon, A., C. E. Dorman, M. A. Merrifield and C. D. Winant, 1991b. The lower atmosphere over the Gulf of California. *Jour. of Geophys. Res.*, **96**, pp. 16877-16896.

Beier, E., 1997. A numerical investigation of the annual variability in the Gulf of California. *Jour. of Phys. Ocean.* (in press).

Bray, N. A., 1988a. Thermohaline circulation in the Gulf of California, *Jour. of Geophys. Res.*, **93**, pp. 4993-5020.

Bray, N. A., 1988b. Water mass formation in the Gulf of California, *Jour. of Geophys. Res.*, **93**, pp. 9223-9240.

Bray, N. A. and J. M. Robles, 1991. Physical oceanography of the Gulf of California. In: The Gulf and Peninsular Provinces of the California's, Chapter 26, pp. 555-567.

Carbajal, N., 1993. Modeling of the circulation in the Gulf of California. Ph.D. thesis, Institute fur Meerskunde, Hamburg, 186 pp.

Christensen, N., R. V. de la Paz and G. Gutiérrez V., 1983. A study of sub-inertial waves off the coast of Mexico. *Deep Sea Research*, **30**, pp. 835-850.

Csanady, G. T., 1984. Circulation in the Coastal Ocean. D. Reidel Company. 279 pp.

Dressler, R., 1981. Investigación sobre mareas y efectos de viento en el Golfo de California, mediante un modelo H-N. Sammlung von Publikationen Dressler. Nr 2, Unpublished Manuscript, 23 pp.

Emilsson, I., and M. A. Alatorre, 1979. Investigaciones recientes sobre la circulación en la parte exterior del Golfo de California. Unpublished manuscript, Centro de Ciencias del Mar y Limnología, Universidad Nacional Autónoma de México, 23 pp.

Fernández-Barajas, M. E., M. A. Monreal-Gómez, A. Molina-Cruz, 1994. Thermohaline structure and geostrophic flow in the Gulf of California, during 1992. *Ciencias Marinas*, **20**, pp. 267-286.

Gill, A. E., 1982. Atmosphere-ocean dynamics. Academic Press, Inc. (London) Ltd., 662 pp.

Godin, G, 1988. Tides. Published by the Centro de Investigacisn Científica y Educación Superior de Ensenada, Ensenada, B. C., México, 287 pp.

Gutiérrez, G. y R. Morales, 1986. Revisión de datos de mareas para el Golfo de California. Reporte Técnico OC- 85-03. Centro de Invesigación Científica y Educación Superior de Ensenada, Ensenada, México, 40 pp.

Hunter, J. R., 1980. User's manual for two-dimensional numerical hydrodynamical model. Unit for the Coastal and Estuarine Studies. Marine Science Laboratories, Menai Bridge, Anglesey. Report U80-5, 23 pp.

Huthnance, J. M., 1973. Tidal current asymmetries over the Norfolk Sandbank. *Estuarine Coastal Marine Sciences* **1**, pp. 89-99.

Huthnance, J. M., 1981. On mass transport generated by tides on long waves. *Jour. of Fluid Mechanics*, **102**, pp. 367-387.

Lavín, M. F., R. Durazo, E. Palacios, M. L. Argote and L. Carrillo, 1997. Lagrangian observations of the circulation in the Northern Gulf of California. *Jour. of Phys. Ocean.* **27**(5), pp 2298-2305.

Lepley, L. K., S. P. Vonder Haar, J. R. Hendrickson and G. Calderón-Riveroll, 1975. Circulation in the northern Gulf of California from orbital photographs and ship investigations. *Ciencias Marinas*, **2**, pp. 86-93.

Marinone, S. G., 1997. A two-dimensional model of tide induced currents in the Gulf of California, México. *Jour. of Geophys. Res.*, **102**, pp. 8611-8623.

Martínez-Sepúlveda, M., 1994. Descripción de la profundidad de la capa mezclada superficial en el Golfo de California. B. Sc. thesis, Facultad de Ciencias Marinas, UABC, Ensenada B. C., México. 48 pp.

Merrifield, M. A., A. Badan-Dangon and C. D. Winant, 1987. Temporal behavior of lower atmospheric variables over the Gulf of California. 1983-1985. A Data Report. SIO Reference Series # 87-6, 192 pp.

Merrifield, M. A. and C. D. Winant, 1989. Shelf circulation in the Gulf of California: a description of the variability. *Jour. of Geophys. Res.*, **94**, pp. 18133-18160.

Navarro-Olache L. F., 1989. Mesoestructuras termohalinas en la parte central del Golfo de California, M. Sc. thesis, Centro de Investigación Científica y de Educación Superior de Ensenada, Ensenada B. C., México.

Organista-Sandoval, S., 1987. Flujos de Calor en el alto Golfo de California, M. Sc. thesis, Centro de Investigación Científica y de Educación Superior de Ensenada, Ensenada B. C., México, 142 pp.

Paden, C. A., M. R. Abbott and C. D. Winant, 1991. Tidal and atmospheric forcing of the upper ocean in the Gulf of California 1. Sea surface temperature variability. *Jour. of Geophys. Res.*, **96**(C10), pp. 18337-18359.

Pingree, R. and L. Maddock, 1977. Tidal residuals in the English Channel. *Jour. of the Marine Biological Association U. K.*, **57** pp 339-354.

Pingree, R., and D. K. Griffiths, 1980. Currents driven by a steady uniform wind stress on the shelf seas around the British Isles. *Oceanológica Acta*, **3**, pp. 227-236.

Quirós, G., A. Badan-Dangon and P. Ripa, 1992. M_2 currents and flow in the Gulf of California. *Netherlands Jour. Sea Res.*, **28**, pp. 251-259.

Reyes-Hernández, A. C. 1993. Efectos de las condiciones atmosféricas de otoño e invierno sobre la formación de masas de agua en el Golfo de California. M. Sc. thesis, Centro de Investigación Científica y Educación Superior de Ensenada, Ensenada B. C., México, 91 pp.

Ripa, P., 1990. Seasonal circulation in the Gulf of California, *Annales Geophysicae*, **8**, 7-8, pp. 559-564.

Ripa, P., 1997. Towards a physical explanation of the seasonal dynamics and thermodynamics of the Gulf of California. *Jour. of Phys. Ocean.* (submitted).

Robinson, I. S., 1983. Tidally induced flows. In Physical oceanography of Coastal and shelf seas (B. John Ed. Elsevier Oceanography Series.), pp. 321-356.

Roden, G. I., 1964. Oceanographic aspects of the Gulf of California, Marine Geology of the Gulf of California: A Symposium, *Mem. Am. Assoc. Pet. Geol.*, **3**, pp. 30-58.

Rosas-Cota, A., 1976. Corrientes geostróficas en el Golfo de California en la superficie y a 200 m durante las estaciones de invierno y verano, California Cooperative Oceanic Fisheries Investigations Report 19, pp. 89-106.

Salas-Pérez, J. J., 1996. El intercambio de agua sobre los umbrales del Golfo de California. M. Sc. thesis, Centro de Investigación Científica y de Educación Superior de Ensenada, B. C., Mexico, Ensenada B. C., México, 142 pp.

Tee, K. T., 1976. Tide-induced currents, a 2-D nonlinear numerical model. *Jour. of Marine Research*, **34**, (4) pp. 603-628

Thomson, D. A., A. R. Mead and J. R. Schreiber, Jr., 1969. Environmental Impact of Brine effluents on Gulf of California, Res. and Dev. Rep. 387, 196 pp., US Dep. of Inter., Washington, D. C.

Zimmerman, J. T. F., 1980. Vorticity transfer by tidal currents over irregular topography, *Jour. of Marine Research*, **38**, pp. 601-630.

List of symbols

C_{10}	=	Drag coefficient for wind stress = 1.3×10^{-3}
C_d	=	Bottom friction coefficient = 3.7×10^{-3}
f	=	Coriolis parameter = 7.7×10^{-5} s^{-1}
g	=	Acceleration due to gravity = 9.81 m s^{-2}
h	=	Water depth measured from the undisturbed free surface
K_h	=	Horizontal eddy viscosity = 10^2 m^2 s^{-1}
T	=	Tidal period = 12.42 h
t	=	Time co-ordinate
U	=	Tidal current amplitude
$\mathbf{u}$	=	Vertical averaged horizontal velocity with components u and v
$\mathbf{u}_e$	=	Eulerian residual mean velocity
$\mathbf{u}(z)$	=	Horizontal velocity at a position z
$\mathbf{W}_{10}$	=	Wind velocity at a high of 10 m = 10.0 m s^{-1}
x, y	=	Horizontal co-ordinates (right hand axes)
z	=	Vertical direction
∇	=	The two dimensional gradient operator
∇_h^2	=	The two dimensional Laplacian operator
η	=	Sea surface elevation
ρ_a	=	Air density = 1.23 kg m^{-3}
ρ_w	=	Water density
σ	=	Frequency of the tidal current = 12.42 h
τ_b	=	Bottom stress
τ_w	=	Wind stress